Improved QRS Complex Detection in Capacitive ECG Measurements through Thick Clothing Using Capacitance Multiplier Circuit

Iori Kudo
Department of Electrical and Electronic Engineering
Tokyo Denki University
Tokyo, Japan
24kmj09@ms.dendai.ac.jp

Akinori Ueno
Department of Electrical and Electronic Engineering
Tokyo Denki University
Tokyo, Japan
0000-0002-5710-1721

***Abstract*—In capacitive electrocardiography (cECG) measurements through thick clothing, signal attenuation in the coupling impedance owing to bulky clothes is a major challenge. This paper presents a capacitance multiplier circuit (CMC) to equivalently amplify the small capacitance of coupling to improve the detection performance of the QRS complex in cECG measurement. We acquired cECG signals using the proposed CMC from five male participants wearing 2.87 mm–thick clothing. The corresponding results reveal that the mean detection rates of sensitivity, accuracy, and positive predictive value exceed 95% by adjusting the amplification factor. Compared with a conventional measurement system without the CMC, the mean accuracy significantly increases by 57.0% ($p < 0.01$), and notable noise mitigation is achieved.**

Keywords—cECG, capacitance multiplier circuit (CMC), QRS complex.

I. Introduction

Cardiovascular diseases are a leading cause of mortality worldwide, accounting for 32% of all global deaths [1]. Of the deaths related to these diseases, those caused by cardiac arrhythmias (CAs) are the most prominent. CAs are disorders characterized by disturbances in the heartbeat caused by electrical conduction anomalies in cardiac muscle [2]. CAs are generally diagnosed through electrocardiography (ECG) recordings. However, CAs occur intermittently at early stages of heart disease, hindering early diagnosis [3]. Consequently, CAs may remain undetected during short-term measurements, rendering long-term monitoring essential to ensure accurate and reliable early diagnosis. Capacitive ECG (cECG) allows acquiring ECG signals through clothing without attaching electrodes directly to the skin. As an unobtrusive technique with minimal physical burden and high applicability to daily living, cECG is suitable for long-term monitoring. Nevertheless, a major challenge in cECG measurement stems from signal attenuation at the coupling impedance caused by clothing. The signal quality deteriorates depending on the thickness and/or resistivity of clothing. This drawback narrows the clothing variety that can be used by different individuals and through seasons. In particular, during winter, thick clothing demands the development of signal acquisition that can overcome such difficult condition.

For cECG signal detection through thick clothing, Nakamura et al. [4] reported successful measurements through 1.7 mm-thick clothing under low humidity using a bootstrapped bandpass amplifier (BPA). In addition, Wang and Lin [5] introduced a negative impedance stage into the detection circuit and reported the successful detection of heartbeat (i.e., QRS complex) through clothing with up to 1.8 mm in thickness. However, neither 1.7 nor 1.8 mm thickness suitably represents the bulky clothing used during cold periods.

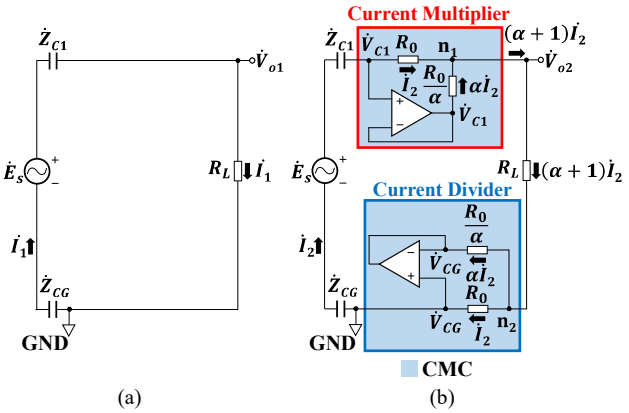

Fig. 1. Schematics of voltage source (E_s) measurement through capacitive couplings (a) without and (b) with CMC, which comprises a current multiplier anacurrent divider.

Alternatively, we focused on a capacitance multiplier circuit (CMC) in this study [6]. To the best of our knowledge, the CMC has not been used for capacitive biopotential sensing. However, it may equivalently amplify the small capacitance formed through thick clothing, thereby mitigating signal attenuation at the coupling impedance. Because the effect of capacitance multiplication on cECG measurements has not been investigated, this study was aimed to determine whether the CMC contributes to the improvement in the detection performance of the QRS complex in cECG signals acquired through thick clothing.

II. Principle of Biopotential Measurement via Capacitive Couplings Using CMC

Fig. 1 shows schematics of the measurement of voltage source $\dot{E}_s$ through capacitive couplings C_1 and C_G using resistive load R_L. In Fig. 1(a), output voltage $\dot{V}_{o1}$ is simply derived from the following voltage division rule:

$$\dot{V}_{o1} = R_L \dot{I}_1 = \frac{R_L}{\dot{Z}_{C1} + \dot{Z}_{CG} + R_L} \dot{E}_s, \qquad (1)$$

where $\dot{Z}_{C1}$ and $\dot{Z}_{CG}$ are the impedances of capacitive couplings C_1 and C_G, respectively.

Fig. 1(b) depicts the CMC composed of a current multiplier and current divider. Assuming an ideal operational amplifier (opamp) of the current multiplier with negative feedback, the opamp output voltage is $\dot{V}_{C1}$ if considering a virtual short. As a result, the potential difference across

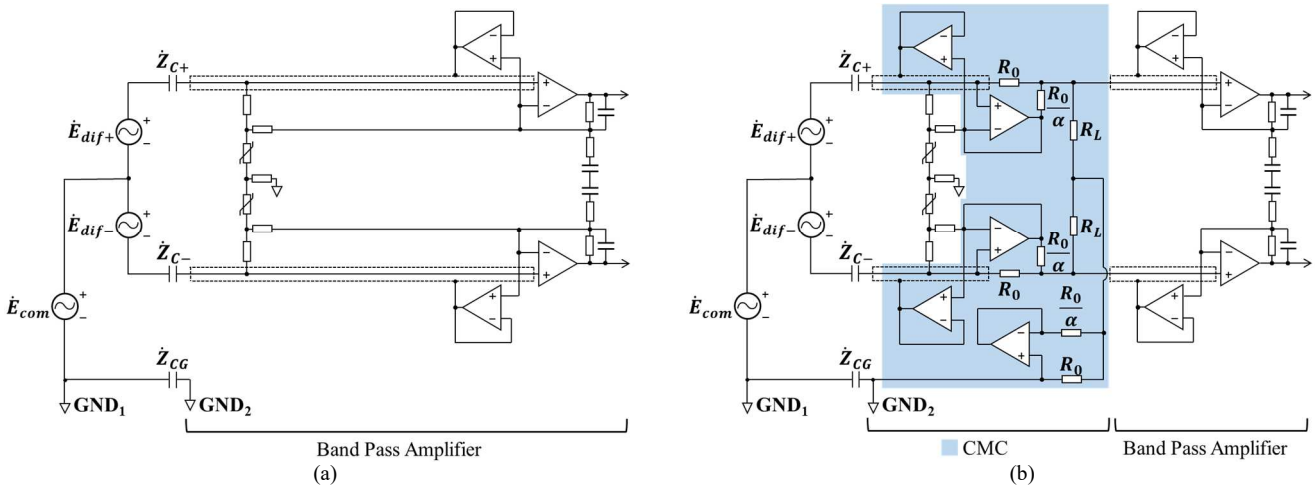

Fig. 2. Front-end differential circuit for cECG measurement (a) without ([4]) and (b) with CMC (proposed).

resistors R_0 and R_0/α become equal to voltage $\dot{V}_{C1} - \dot{V}_{o2}$. Thus, the current through R_0 can be obtained by Ohm's law as follows:

$$\dot{I}_2 = \frac{\dot{V}_{C1} - \dot{V}_{o2}}{R_0}. \tag{2}$$

The current through R_0/α, denoted as $\dot{I}_{(R_0/\alpha)}$, can be obtained as follows:

$$\dot{I}_{(R_0/\alpha)} = \frac{\dot{V}_{C1} - V_{o2}}{\frac{R_0}{\alpha}} = \alpha\frac{\dot{V}_{C1} - V_{o2}}{R_0} = \alpha\dot{I}_2. \tag{3}$$

The currents given by (2) and (3) join at node n_1. Hence, current $(\alpha+1)\dot{I}_2$ flows through load resistance R_L.

Considering the current divider, the output voltage of an opamp becomes $\dot{V}_{CG}(=0)$ according to the virtual short. Therefore, the potential difference across resistors R_0/α and R_0 become equal to $\dot{V}_{\mathrm{n2}} - 0$. As a result, the current entering node n_2, $(\alpha+1)\dot{I}_2$, is divided into $\alpha\dot{I}_2$ and $\dot{I}_2$ for resistors R_0/α and R_0, respectively.

From Fig. 1(b), according to Kirchhoff's and Ohm's laws, we obtain

$$-\dot{Z}_{CG}\dot{I}_2 + \dot{E}_s - \dot{Z}_{C1}\dot{I}_2 - R_0\dot{I}_2 - (\alpha+1)R_L\dot{I}_2 - R_0\dot{I}_2 = 0. \tag{4}$$

Rearranging (4), current $\dot{I}$ can be expressed as

$$\dot{I}_2 = \frac{\dot{E}_s}{\dot{Z}_{C1} + \dot{Z}_{CG} + 2R_0 + (\alpha+1)R_L}. \tag{5}$$

Combining (5) and Ohm's law, output voltage $\dot{V}_{o2}$ is given by

$$\begin{aligned}\dot{V}_{o2} &= (\alpha+1)R_L\dot{I}_2 + R_0\dot{I}_2 \\ &= \frac{(\alpha+1)R_L + R_0}{\dot{Z}_{C1} + \dot{Z}_{CG} + 2R_0 + (\alpha+1)R_L}\dot{E}_s \\ &= \frac{R_L + \frac{1}{\alpha+1}R_0}{\frac{\dot{Z}_{C1} + \dot{Z}_{CG}}{\alpha+1} + \frac{2}{\alpha+1}R_0 + R_L}\dot{E}_s. \end{aligned} \tag{6}$$

When $2R_0/(\alpha+1) \ll R_L$, (6) can be approximated as

$$\dot{V}_{o2} \approx \frac{R_L}{\frac{\dot{Z}_{C1} + \dot{Z}_{CG}}{\alpha+1} + R_L}\dot{E}_s. \tag{7}$$

Comparing (7) with (1), coupling impedances $\dot{Z}_{C1} = 1/(\omega C_1)$ and $\dot{Z}_{CG} = 1/(\omega C_G)$ seem equivalently decreased by factor $(\alpha+1)$ when using the CMC. Therefore, coupling capacitances C_1 and C_G can be considered as multiplied by $(\alpha+1)$.

Fig. 2 shows the fully differential front-end detection circuits for cECG measurement adopted for evaluation with human participants. Fig. 2(a) shows an existing BPA without the CMC [4]. Fig. 2(b) shows the fully differential CMC introduced before the BPA.

III. Materials and Methods

A. cECG Measurement System and Experimental Setup

Fig. 3 shows the experimental setup and block diagrams of the cECG measurement system for CMC parameter adjustment (section III-B) and performance evaluation with human participants (section III-C). In Fig. 3(a), the cECG signal is measured through capacitive couplings composed of actual capacitors. The measurement system comprises the fully differential CMC, BPA, AC coupling circuit, and instrumentation amplifier with DC suppression. The frequency band and total gain of the system are set to 0.5–50 Hz and 150 V/V, respectively.

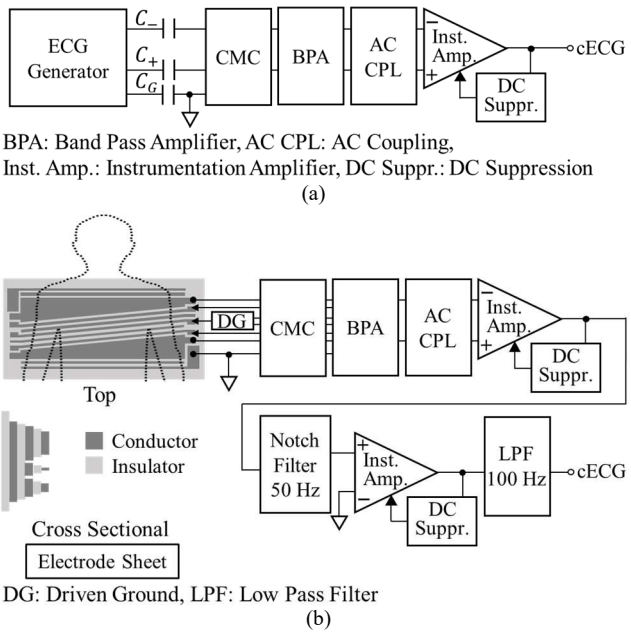

Fig. 3. Block diagram of cECG measurement system through (a) capacitor elements with small capacitance (47 pF) and (b) thick (2.87 mm) clothing from human participant lying on electrode sheet. The electrode sheet is placed under a bedsheet (0.35-mm thick).

In Fig. 3(b), the cECG signal is measured through thick clothing from a human participant lying on a multilayered electrode sheet and using the measurement system. In addition to the system shown in Fig. 3(a), a notch filter, instrumentation amplifier with DC suppression, and lowpass filter are introduced. The frequency band and total gain of the system are set to 0.7–40 Hz and 720 V/V, respectively. The electrode sheet comprises three conductive layers (i.e., sensing, guard, and ground) and two insulating layers between them. The trapezoidal shape of the sensing layer contributes to a high detection rate (>95%) of cECG P-wave through 1.0 mm–thick clothing [7]. The drive ground circuit shown in Fig. 3(b) is intended to suppress common-mode noise and shorten the baseline restoration time [8]. The measured cECG signals are digitized at 1.0 kHz with 16-bit resolution between −10 and +10 V using a BIOPAC Systems MP150 analog-to–digital converter and recorded on a personal computer.

B. Parameter Adjustment in CMC for Sensitive and Stable cECG Measurement

To evaluate the influence of CMC parameter α, which represents current amplification factor, on sensitive and stable cECG measurement, experiments were conducted at different α values using a fixed capacitive coupling with small capacitance (47 pF). Parameter α was set to 1, 1000, 5000, 10,000, and 50,000. A pseudo-ECG generator (AX-301D, NIHON KODEN) was used as the signal source. The amplitude and heartrate of the pseudo-ECG were 1 mV and 60 bpm, respectively. The 47 pF capacitance of the couplings was selected to be below the 57 pF reported for 1.8 mm–thick clothing [5]. For reference, direct signal from the pseudo-ECG generator (ECG_{ref}) was simultaneously measured with a BIOPAC Systems BN-ECG2 telemetry system.

C. Evaluation of CMC in cECG Measurement from Human Participants

All experimental procedures were approved by the Human Life Ethics Committee of Tokyo Denki University. Five healthy males (weight of 71.0 ± 12.0 kg, height of 173.2 ± 5.8 cm, body mass index of 23.6 ± 2.9), who provided informed consent, participated in the experiment. To compare the QRS detection performance of the measurement systems without and with the CMC (α = 10,000 A/A), cECG signals were acquired from the participant's back using the electrode sheet. All participants wore three layers of clothing: underwear (0.46-mm thick), long-sleeve T-shirt (0.66-mm thick), and long-sleeve sweatshirt (1.40-mm thick). Every participant lay in the supine position on the electrode sheet, which was placed on a commercial examination table and covered with a cotton bedsheet (0.35-mm thick). All clothing and the bedsheet were made of cotton, and their total thickness was 2.87 mm.

The cECG signals were measured for 5 min and twice per system under moderate humidity (44.2% ± 1.2%, 10.1 ± 0.3 g/m^3). Reference signal + of lead II ECG (ECG_{ref}) was measured with the same telemetry system described in section III-B using disposable electrodes (F-150S, Nihon Kohden). As a preprocessing step, cECG and ECG_{ref} signals were smoothed by applying a 20-point moving average. The measured voltage of cECG and ECG_{ref} signals were converted into input-referred volage and then processed by applying an infinite impulse response bandpass filter (0.5–40 Hz) and differentiation (10 points).

The BIOPAC Systems AcqKnowledge 4.1 software was used for analysis. The QRS complex was detected on a 3 min segment 2 min after the measurement onset using a threshold for the preprocessed signals. The threshold was set to 60% of the larger mean absolute value of positive or negative amplitude of the QRS complexes in the first 10 heartbeats of the segment. The peak or trough for detection was determined based on the mean of absolute value of the QRS complexes in the ECG_{ref} signal.

When the peak or trough time of the QRS complex in cECG signal was within ±10 ms with respect to that of the ECG_{ref} signal, the QRS complex of the cECG signal was deemed correctly detected. The sensitivity (P_{SNS}), accuracy (P_{ACC}), and positive predictive value (P_{PPV}) of the detected QRS complexes in the cECG measurements were calculated using (8)–(10), respectively:

$$P_{SNS} = \frac{N_{TP}}{N_{TP} + N_{FP}} \times 100, \tag{8}$$

$$P_{ACC} = \frac{N_{TP} + N_{TN}}{N_{TP} + N_{TN} + N_{FP} + N_{FN}} \times 100, \tag{9}$$

$$P_{PPV} = \frac{N_{TP}}{N_{TP} + N_{FN}} \times 100, \tag{10}$$

where N_{TP}, N_{FP}, and N_{FN} are the numbers of QRS complexes correctly detected (true positives), falsely detected (false positives), and undetected (false negatives), respectively. Given the lack of countable valid events corresponding to N_{TN}, it was set to zero when calculating the accuracy. The mean was calculated for the system without or with the CMC and for every participant.

IV. Results and Discussion

A. Parameter Adjustment in CMC for Sensitive and Stable cECG Measurement

Fig. 4 shows the ECG_{ref} and cECG signals obtained at different α values for the CMC. The correlation between two signals was the lowest (r = 0.441) at α = 1 A/A (Fig. 4(a)) and highest (r = 0.790) at α = 10,000 A/A (Fig. 4(b)). These results confirm that signal distortion and noise were reduced by increasing α. The reduction in distortion and noise was attributed to the amplification of the weak current flowing through capacitive couplings by the CMC. Such amplification may have increased the fraction of voltage depression across resistive load R_L in the loop shown in Figs. 1 and 2 compared with that across the capacitive couplings.

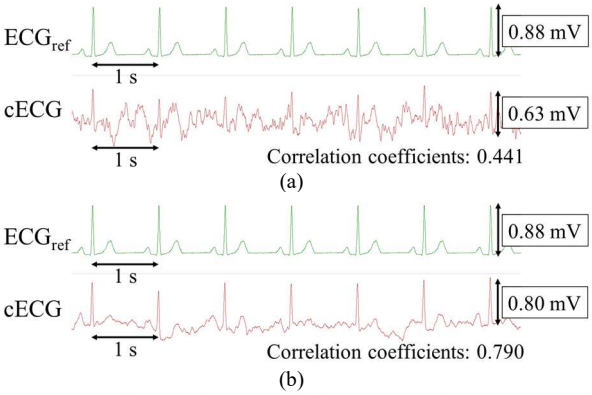

Fig. 4. cECG and ECG_{ref} signals for different CMC gains of (a) α = 1 A/A and (b) α = 10,000 A/A. Measurements were acquired through an off-the-shelf capacitor of 47 pF. The capacitance of 47 pF for the couplings was <57 pF capacitance reported for 1.8 mm-thick clothing [5].

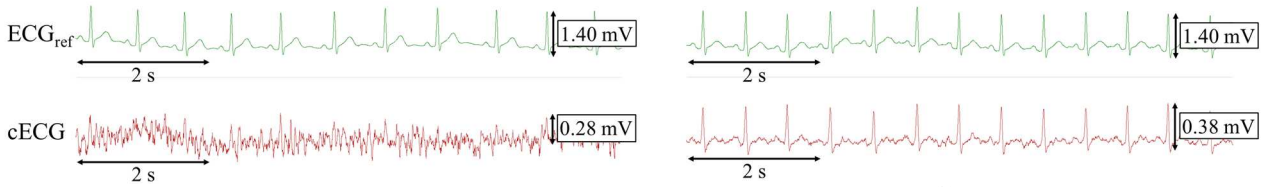

Fig. 5. Comparison of cECG signals obtained from participant #1 (a) without and (b) with CMC. The measurements were acquired through cotton clothing with a total thickness of 2.87 mm and volume absolute humidity of 10.1 g/m³.

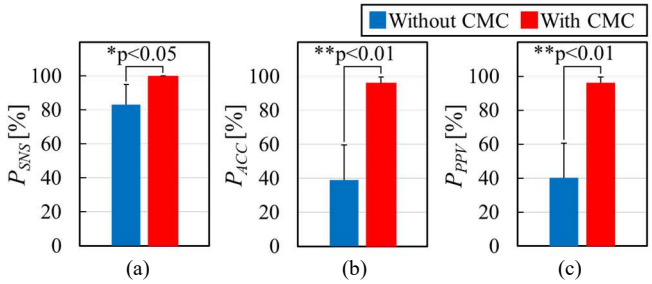

Fig. 6. Comparison of (a) sensitivity (P_{SNS}), (b) accuracy (P_{ACC}), and (c) positive predictive value (P_{PPV}) of QRS complex detection without and with CMC. Significant differences were observed in sensitivity ($p < 0.05$), accuracy ($p < 0.01$), and positive predictive value ($p < 0.01$).

Meanwhile, increasing α from 10,000 to 50,000 A/A slightly decreased the correlation from 0.790 to 0.753 (these signals are not shown). This may have been because the CMC amplifies the entire frequency band, causing the amplitude of low-frequency components outside the ECG wave band to become very large. This may lead to waveform distortion and degradation of cECG recordings, thus reducing the signal correlation to the ECG$_{ref}$ recordings.

Concerning P_{ACC} of QRS complex, cECG signals at α = 1 and 10,000 showed 100%. Fixing α value at 10,000 and reducing the coupling capacitance in Fig. 3(a) from 47 to 22 pF and then to 15 pF, P_{ACC} gradually decreased from 100% to 64.0% and to 36.8% respectively. Therefore, coupling capacitance that leads to P_{ACC} = 50% is assumed to be 18 pF.

B. Evaluation of CMC in cECG Measurement from Human Participants

Fig. 5 shows simultaneous recordings of ECG$_{ref}$ and cECG for participant 1 without and with the CMC. In Fig. 5(a), large noise comparable with the QRS complexes of ECG was superimposed throughout the recording. Consequently, it was difficult to distinguish the QRS complexes from noise. In contrast, Fig. 5(b) shows that noise was greatly mitigated, and distinct QRS complexes were observed.

Fig. 6 shows that all mean detection rates of P_{SNS}, P_{ACC}, and P_{PPV} exceeded 95% when using the CMC, being significantly higher than those without the CMC. Particularly, P_{SNS}, P_{ACC}, and P_{PPV} improved by 16.8%, 57.0%, and 55.9%, respectively (paired t-test). As listed in Table I, P_{ACC} exceeded 95% in four of five participants when using the CMC. These improvements were attributed to the significant noise reduction achieved by the CMC.

In this study, all participants were male and within a normal BMI range. Therefore, future studies will include participants with a wider BMI range, including females.

V. Conclusion

We evaluated whether the introduction of a CMC improved the detection of the QRS complex in cECG signals acquired through 2.87 mm–thick clothing. The cECG signals acquired from five healthy male participants in the supine position showed that cECG detection using the proposed CMC achieved significant improvements by 16.8% in sensitivity ($p < 0.05$), 57.0% in accuracy ($p < 0.01$), and 55.9% in positive predictive value ($p < 0.01$). Future studies should evaluate the use of various clothing materials such as chemical fiber fabrics. In addition, the cECG measuring system can be further improved to ensure stable detection of T- and P-waves through thick clothing.

TABLE I. Accuracy, Sensitivity, and Positive Predictive Value of QRS Complex Detection without and with CMC.

Participant ID	P_{SNS} [%]		P_{ACC} [%]		P_{PPV} [%]	
	Without CMC	*With CMC*	*Without CMC*	*With CMC*	*Without CMC*	*With CMC*
#1	73.6	100	19.1	99.8	21.4	99.8
#2	98.7	100	52.5	95.7	53.2	95.7
#3	65.9	99.3	9.6	89.8	10.1	90.4
#4	91.4	99.7	57.9	96.4	59.0	96.6
#5	85.6	100	56.5	98.6	57.6	98.6
Mean	83.0	99.8	39.1	96.1	40.3	96.2

Acknowledgement

This research was partially supported by the Research Institute for Science and Technology of Tokyo Denki University and partially by the Fukuda Foundation for Medical Technology.

References

[1] World Health Organization, “Cardiovascular diseases (CVDs)” WHO, Jun. 11, 2020. [Online]. Available: https://www.who.int/news-room/fact-sheets/detail/cardiovascular-diseases-(cvds).

[2] Y. D. Daydulo, B. L. Thamineni, and A. A. Dawud, “Cardiac arrhythmia detection using deep learning approach and time frequency representation of ECG signals,” BMC Med. Informat. Decis. Making, vol. 23, no. 1, Art. no. 232, 2023.

[3] J. A. Gutiérrez-Gnecchi, R. Morfin-Magaña, and D. Lorias-Espinoza, et al.,“DSP-based arrhythmia classification using wavelet transform and probabilistic neural network,” Biomed. Sign. Proc. Contr, vol. 32, pp. 44–56, 2017.

[4] H. Nakamura, Y. Sakajiri, H. Ishigami and A. Ueno, “A novel analog front end with voltage-dependent input impedance and bandpass amplification for capacitive biopotential measurements,” Sensors, vol. 20, no. 9, pp. 1–18, PID #2476, Apr. 2020.

[5] T. W. Wang and S. F. Lin, “Negative Impedance Capacitive Electrode for ECG Sensing Through Fabric Layer,” IEEE Trans. Instrum. Meas., vol. 70, pp. 1-8, 2021.

[6] H. Ito, T. Terashima, and N. Imai, “An improvement of the temperature characteristics of driving circuit for humidity sensor using both a Negative-Capacitor-Circuit and a Capacitance-Scaling-Circuit,” IEEJ Trans. Electr. Inf. Syst., vol. 114, issue 5, pp. 609-610, 1994. (in Japanese).

[7] I. Kudo and A. Ueno, “Evaluation of p-Wave Detection Capability of Capacitive Electrocardiogram Measurement System with Electrode Sheet,” IEEE BSN, pp. 1-4, 2024.

[8] M. Takano and A. Ueno, “Noncontact in-bed measurements of physiological and behavioral signals using an integrated fabric-sheet sensing scheme,” IEEE J. Biomed. Health Inf., vol. 23, no.2, pp.618–630, March 2019.